Quadcopter UAV Modeling and Automatic Flight Control Design

Bhatia Ajeet Kumar[1*], *Jiang Ju*[1,2], *Zhen Ziyang*[1,2]

1. College of Automation Engineering, Nanjing University of Aeronautics and Astronautics, Nanjing 210016, P. R. China;
2. Jiangsu Key Laboratory of Internet of Things and Control Technologies, Nanjing 210016, P. R. China

(Received 18 November 2015; revised 2 January 2016; accepted 12 April 2016)

Abstract: The mathematical model of quadcopter-unmanned aerial vehicle (UAV) is derived by using two approaches: One is the Newton-Euler approach which is formulated using classical mechanics; and other is the Euler-Lagrange approach which describes the model in terms of kinetic (translational and rotational) and potential energy. The proposed quadcopter's non-linear model is incorporated with aero-dynamical forces generated by air resistance, which helps aircraft to exhibits more realistic behavior while hovering. Based on the obtained model, the suitable control strategy is developed, under which two effective flight control systems are developed. Each control system is created by cascading the proportional-derivative (PD) and T-S fuzzy controllers that are equipped with six and twelve feedback signals individually respectively to ensure better tracking, stabilization, and response. Both proposed flight control designs are then implemented with the quadcopter model respectively and multitudinous simulations are conducted using MATLAB/Simulink to analyze the tracking performance of the quadcopter model at various reference inputs and trajectories.

Key words: quadcopter; unmanned aerial vehicle (UAV); flight control design; T-S fuzzy inference system; proportional-derivative (PD) controller

CLC number: V249 **Document code**: A **Article ID**: 1005-1120(2017)06-0627-10

0 Introduction

A quadcopter, also referred as a rotorcraft, is a type of helicopter that has four independent rotors, two of which spin clockwise and other two spin counterclockwise. The rotors are directed upwards and they are fixed in a square formation with identical distance from the center of mass of the quadcopter. The rotors are spun rapidly to push air downwards, consequently producing a thrust force that lifts the quadcopter. As quadcopters are capable of vertical take-off and landing (VTOL) and do not require any complex mechanical linkages, such as swash plates or teeter hinges that ordinarily appear in typical helicopters[1,2]. Because of its simple mechanical structure, it has been envisioned for various applications, such as investigation, surveillance, search, rescue, construction, mobile sensory networks, as well as educational purposes and so on[2].

The quadcopter is maneuvered by regulating the angular velocities of its four rotors which are spun by electrical motors. Each rotor produces thrust and torque forces, whose combination generates the main thrust and the yaw, pitch, roll torques acting on the quadcopter.

Designing a full control system for a quadcopter is a fundamentally challenging and interesting problem. With six degrees of freedom (6-DOF) (three translational and three rotational) and only four independent inputs (rotor speeds), this is severely under-actuated system. Additionally, the rotational and translational motions are coupled, resulting in a highly nonlinear dynamics, particularly after accounting for the complicated aerodynamic effects[3,4]. Finally, unlike the ground vehicles, unmanned aerial vehicles (UA-

* Corresponding author, E-mail address: zhenziyang@nuaa.edu.cn.

How to cite this article: Bhatia Ajeet Kumar, Jiang Ju, Zhen Ziyang. Quadcopter UAV modeling and automatic flight control design[J]. Trans. Nanjing Univ. Aero. Astro., 2017,34(6):627-636.
http://dx.doi.org/10.16356/j.1005-1120.2017.06.627

Vs) have very low friction to thwart their motion, so they must provide their own damping in order to stop moving and stay stable. Together, these factors craft very exciting control problems[3,5].

In this paper, the proportional-derivative (PD) and T-S fuzzy controllers are used to design the control system for quadcopter. Fuzzy logic is being used to control or define a system by using commonsensical rules that refer to inadequate quantities. It combines a simple rule-based if-then approach to solve a control problem rather than attempting to model a system mathematically. Thanks to the use of linguistic information, stimulation of human thinking and the capability of compensating the estimated and imprecise nature of the real world, fuzzy rule-based systems are said to perform very efficiently in a wide variety of practical problems[6-8].

We present an effective flight control design for a highly nonlinear quadcopter model that is tested by conducting numerous simulations using MATLAB/Simulink.

1 Quadcopter Modelling and Control

1.1 Kinematics

The quadcopter is an aerial vehicle so its kinematics can be derived in two frames in which it will operate. The first is supposed as an inertial frame which is fixed with the ground, with gravitational force g pointing in the negative z-direction, as shown in Fig. 1. And the second is the body frame which is fixed with a quadcopter that describes the angular position or orientation of the quadcopter, with the rotor axes pointing in the positive z-direction and the arms pointing in the x and y-directions[1-5,9-22]. As shown in Fig. 1, the origin of the body frame is at the center of mass of the quadcopter and x-axis lies along the arm of motor-1 (spins counter-clockwise) and the y-axis is set along the arm of motor-4 (spins clockwise) and the z-axis pointing upwards.

The absolute linear position $\boldsymbol{\xi}_I$ of the quadcopter is defined in the inertial frame with x, y and z-axes. The attitude, i. e. the angular posi-

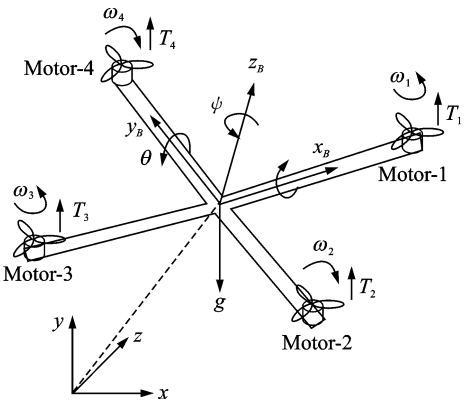

Fig. 1 Quadcopter in inertial and body frame

tion $\boldsymbol{\eta}_I$ in the inertial frame is defined by three Euler angles, which are the roll angle φ, the pitch angle θ, and the yaw angle ψ, expounding the gyration of the quadcopter the y-axis, x-axis and the z-axis, respectively[1,2]

$$\boldsymbol{\xi}_I = \begin{bmatrix} x \\ y \\ z \end{bmatrix}, \quad \boldsymbol{\eta}_I = \begin{bmatrix} \varphi \\ \theta \\ \psi \end{bmatrix}, \quad \boldsymbol{\varepsilon}_I = \begin{bmatrix} \xi_I \\ \eta_I \end{bmatrix} \tag{1}$$

In the body frame, the linear velocities are defined by the vector $\boldsymbol{S}_B$ and the angular velocities by $\boldsymbol{\Omega}_B$.

$$\boldsymbol{S}_B = \begin{bmatrix} K \\ L \\ M \end{bmatrix}, \quad \boldsymbol{\Omega}_B = \begin{bmatrix} p \\ q \\ r \end{bmatrix} \tag{2}$$

where K, L and M are linear velocities and p, q and r the angular velocities in x, y and z-axes, respectively.

The rotational matrix transforms the linear and the angular positions from body frame to the inertial frame is given as

$$\boldsymbol{R} = \begin{bmatrix} C_\psi C_\theta & C_\psi S_\theta S_\varphi - S_\psi C_\varphi & C_\psi S_\theta C_\varphi + S_\psi S_\varphi \\ S_\psi C_\theta & S_\psi S_\theta S_\varphi + C_\psi C_\varphi & S_\psi S_\theta C_\varphi - C_\psi S_\varphi \\ -S_\theta & C_\theta S_\varphi & C_\theta C_\varphi \end{bmatrix} \tag{3}$$

where $S_{(\cdot)} = \sin(\cdot)$ and $C_{(\cdot)} = \cos(\cdot)$. The rotation matrix $\boldsymbol{R}$ is orthogonal, hence $\boldsymbol{R}^{-1} = \boldsymbol{R}^{\mathrm{T}}$ is the rotation matrix that transforms position parameters from the inertial frame to the body frame.

The transformation matrix $\boldsymbol{W}_\eta$ is to transform the angular velocities from the inertial frame to the body frame and vice versa, as shown below

$$\dot{\boldsymbol{\eta}}_I = \boldsymbol{W}_\eta^{-1} \boldsymbol{\Omega}_B, \quad \begin{bmatrix} \dot{\varphi} \\ \dot{\theta} \\ \dot{\psi} \end{bmatrix} = \begin{bmatrix} 1 & S_\varphi T_\theta & C_\varphi T_\theta \\ 0 & C_\varphi & -S_\varphi \\ 0 & \dfrac{S_\varphi}{C_\theta} & \dfrac{C_\varphi}{C_\theta} \end{bmatrix} \cdot \begin{bmatrix} p \\ q \\ r \end{bmatrix} \tag{4}$$

$$\boldsymbol{\Omega}_B = \boldsymbol{W}_\eta \cdot \dot{\boldsymbol{\eta}}_I, \quad \begin{bmatrix} p \\ q \\ r \end{bmatrix} = \begin{bmatrix} 1 & 0 & -S_\theta \\ 0 & C_\varphi & C_\theta S_\varphi \\ 0 & -S_\varphi & C_\theta C_\varphi \end{bmatrix} \cdot \begin{bmatrix} \dot{\varphi} \\ \dot{\theta} \\ \dot{\psi} \end{bmatrix} \tag{5}$$

where $T_{(\cdot)} = \tan(\cdot)$. The matrix $\boldsymbol{W}_\eta$ is invertible if $\theta \neq (2a-1)\varphi/2, a \in \boldsymbol{Z}$.

The inertia matrix $\boldsymbol{I}$ describes the quadcopter's mass moment of inertia across the defined axes and it is important to the dynamics of the system. Due to the symmetric structure of quadcopter, the inertia matrix $\boldsymbol{I}$ is a diagonal matrix

$$\boldsymbol{I} = \begin{bmatrix} I_{xx} & 0 & 0 \\ 0 & I_{yy} & 0 \\ 0 & 0 & I_{zz} \end{bmatrix} \tag{6}$$

where $\boldsymbol{I}_{xx} = \boldsymbol{I}_{yy}$.

1.2 Dynamics

The angular velocity and acceleration of the ith rotor, denoted by ω_i and $\dot{\omega}_i$, respectively, produce a thrust force T_i in the direction of the rotor axis and torque force τ_{mi} in the direction of rotor axis[2]

$$T_i = k\omega_i^2, \quad \tau_{mi} = b\omega_i^2 + I_m\dot{\omega}_i \tag{7}$$

where k is the lift constant, b the drag constant, I_m the inertia of the motor and $i = 1, \cdots, 4$.

Generally, the effect of $\dot{\omega}_i$ is very small and therefore it can be nullified. The combined forces of rotors create the net thrust $\boldsymbol{T}_B$ in z-axis direction and the torque τ_B in the direction of the corresponding axes in the body frame, as shown in Eqs. (8) and (9), respectively

$$\boldsymbol{T}_B = \begin{bmatrix} 0 \\ 0 \\ T \end{bmatrix}, \quad T = \sum_{i=1}^{4} T_i = k\sum_{i=1}^{4}\omega_i^2 \tag{8}$$

$$\boldsymbol{\tau}_B = \begin{bmatrix} \tau_\varphi \\ \tau_\theta \\ \tau_\psi \end{bmatrix} = \begin{bmatrix} lk(\omega_4^2 - \omega_2^2) \\ lk(\omega_3^2 - \omega_1^2) \\ \sum_{i=1}^{4}\tau_{mi} \end{bmatrix} = \begin{bmatrix} lk(\omega_4^2 - \omega_2^2) \\ lk(\omega_3^2 - \omega_1^2) \\ b(\omega_4^2 + \omega_2^2 - \omega_3^2 - \omega_1^2) \end{bmatrix} \tag{9}$$

where l is the distance between the rotor and the center of gravity of the quadcopter.

From Eqs. (8), (9) it is very clear that the roll motion can be acquired by decreasing ω_2 and increasing ω_4. Similarly, the pitch motion is acquired by decreasing ω_1 and increasing ω_3. Yaw motion is acquired by increasing the angular velocities of two opposite rotors and decreasing the velocities of the other two. By adjusting three torques presented in Eq. (9) and total thrust presented in Eq. (8), the quadcopter can be maneuvered as shown in Fig. 2.

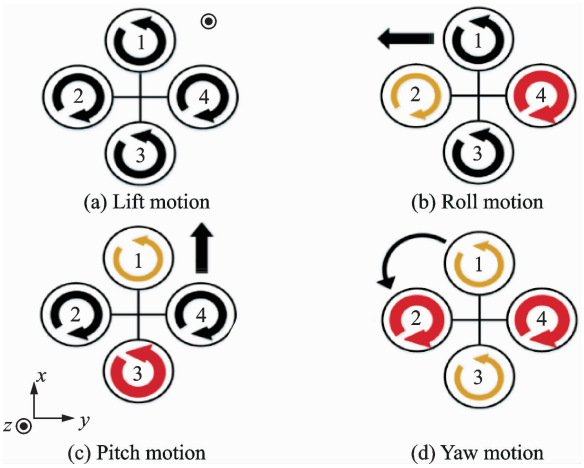

Fig. 2 Quadcopter dynamics

1.3 Newton-Euler approach

The general motion of a rigid body in space is a combination of translational and rotational motions. The quadcopter is assumed to be the rigid body and hence, Newton-Euler equations can be used to describe its dynamics. Using the Newton-Euler formalism, the translational motion of quadcopter in body frame can be given by force balance equation as[2,15]

$$m\boldsymbol{S}_B + s \times (m\boldsymbol{S}_B) = \boldsymbol{R}^{\mathrm{T}} g + \boldsymbol{T}_B \tag{10}$$

where m is the mass of the quadcopter and $s \times (m\boldsymbol{S}_B)$ the centrifugal force.

The linear acceleration in the inertial frame is given as

$$m\ddot{\boldsymbol{\xi}}_I = -mg + \boldsymbol{R}\boldsymbol{T}_B \tag{11}$$

$$\begin{bmatrix} \ddot{x} \\ \ddot{y} \\ \ddot{z} \end{bmatrix} = -g\begin{bmatrix} 0 \\ 0 \\ 1 \end{bmatrix} + \frac{\boldsymbol{T}}{m}\begin{bmatrix} S_\theta C_\varphi C_\psi + S_\varphi S_\psi \\ S_\theta C_\varphi S_\psi - S_\varphi C_\psi \\ C_\theta C_\varphi \end{bmatrix} \tag{12}$$

In the body frame, the rotational motion of quadcopter is presented by its torque balance equation, given as

$$\boldsymbol{I}\dot{\boldsymbol{\Omega}}_B + \boldsymbol{\Omega}_B \times (\boldsymbol{I}\boldsymbol{\Omega}_B) + \boldsymbol{\Pi} = \tau_B \tag{13}$$

where $\boldsymbol{\Pi} = \boldsymbol{I}_m\boldsymbol{\Omega}_B \times \begin{bmatrix} 0 \\ 0 \\ 1 \end{bmatrix}\omega_\Pi$.

$$\begin{bmatrix}\dot{p}\\ \dot{q}\\ \dot{r}\end{bmatrix}=\begin{bmatrix}\dfrac{(I_{yy}-I_{zz})qr}{I_{xx}}\\ \dfrac{(I_{zz}-I_{xx})pr}{I_{yy}}\\ \dfrac{(I_{xx}-I_{yy})pq}{I_{zz}}\end{bmatrix}-\boldsymbol{I}_m\begin{bmatrix}\dfrac{q}{I_{xx}}\\ \dfrac{-p}{I_{yy}}\\ 0\end{bmatrix}\omega_{\Pi}+\begin{bmatrix}\dfrac{\tau_{\varphi}}{I_{xx}}\\ \dfrac{\tau_{\theta}}{I_{yy}}\\ \dfrac{\tau_{\psi}}{I_{zz}}\end{bmatrix} \tag{14}$$

where $\omega_{\Pi}=\omega_4+\omega_2-\omega_3-\omega_1$ is resulting from the gyroscopic precession. Then the angular acceleration in the inertial frame is given as

$$\ddot{\boldsymbol{\eta}}_I=\frac{\mathrm{d}}{\mathrm{d}t}(\boldsymbol{W}_{\eta}^{-1}\boldsymbol{\Omega}_B)=\dot{\boldsymbol{W}}_{\eta}^{-1}\boldsymbol{\Omega}_B+\boldsymbol{W}_{\eta}^{-1}\dot{\boldsymbol{\Omega}}_B \tag{15}$$

$$\begin{bmatrix}\ddot{\varphi}\\ \ddot{\theta}\\ \ddot{\psi}\end{bmatrix}=\begin{bmatrix}0 & \dot{\varphi}C_{\varphi}T_{\theta}+\dfrac{\dot{\theta}S_{\varphi}}{C_{\theta}^2} & -\dot{\varphi}S_{\varphi}C_{\theta}+\dfrac{\dot{\theta}C_{\varphi}}{C_{\theta}^2}\\ 0 & -\dot{\varphi}S_{\varphi} & -\dot{\varphi}C_{\varphi}\\ 0 & \dfrac{\dot{\varphi}C_{\varphi}}{C_{\theta}}+\dfrac{\dot{\varphi}S_{\varphi}T_{\theta}}{C_{\theta}} & -\dfrac{\dot{\varphi}S_{\varphi}}{C_{\theta}}+\dfrac{\dot{\theta}C_{\varphi}T_{\theta}}{C_{\theta}}\end{bmatrix}\begin{bmatrix}p\\ q\\ r\end{bmatrix}+\begin{bmatrix}1 & S_{\varphi}T_{\theta} & C_{\varphi}T_{\theta}\\ 0 & C_{\varphi} & -S_{\varphi}\\ 0 & \dfrac{S_{\varphi}}{C_{\theta}} & \dfrac{C_{\varphi}}{C_{\theta}}\end{bmatrix}\begin{bmatrix}\dot{p}\\ \dot{q}\\ \dot{r}\end{bmatrix} \tag{16}$$

The quadcopter′s dynamical equations that representing 6-DOF can be written as

$$\begin{cases}\ddot{x}=\dfrac{T}{m}(S_{\theta}C_{\varphi}C_{\psi}+S_{\varphi}S_{\psi})\\ \ddot{y}=\dfrac{T}{m}(S_{\theta}C_{\varphi}S_{\psi}-S_{\varphi}C_{\psi})\\ \ddot{z}=\dfrac{T}{m}(C_{\theta}C_{\varphi})-g\\ \ddot{\varphi}=q\left(\dot{\varphi}C_{\varphi}T_{\theta}+\dfrac{\dot{\theta}S_{\varphi}}{C_{\theta}^2}\right)+r\left(-\dot{\varphi}S_{\varphi}C_{\theta}+\dfrac{\dot{\theta}C_{\varphi}}{C_{\theta}^2}\right)+\\ \qquad\dot{p}+\dot{q}S_{\varphi}T_{\theta}+\dot{r}C_{\varphi}T_{\theta}\\ \ddot{\theta}=-q\dot{\varphi}S_{\varphi}-r\dot{\varphi}C_{\varphi}+\dot{q}C_{\varphi}-\dot{r}S_{\varphi}\\ \ddot{\psi}=q\left(\dfrac{\dot{\varphi}C_{\varphi}}{C_{\theta}}+\dfrac{\dot{\varphi}S_{\varphi}T_{\theta}}{C_{\theta}}\right)+r\left(-\dfrac{\dot{\varphi}S_{\varphi}}{C_{\theta}}+\dfrac{\dot{\theta}C_{\varphi}T_{\theta}}{C_{\theta}}\right)+\\ \qquad\dot{q}\left(\dfrac{S_{\varphi}}{C_{\theta}}\right)+\dot{r}\left(\dfrac{C_{\varphi}}{C_{\theta}}\right)\end{cases} \tag{17}$$

1.4 Euler-Lagrange approach

Lagrange approach presents the dynamics of quadcopter in terms of energies (kinetic and potential energy)[1,2,5,9,13]

$$\boldsymbol{L}(\varepsilon,\dot{\varepsilon})=\boldsymbol{E}_{\mathrm{trans}}+\boldsymbol{E}_{\mathrm{rot}}-\boldsymbol{E}_{\mathrm{pot}} \tag{18}$$

where $\boldsymbol{E}_{\mathrm{trans}}=\dfrac{m}{2}\dot{\boldsymbol{\xi}}_I^{\mathrm{T}}\dot{\boldsymbol{\xi}}_I$ is the translational kinetic energy, $\boldsymbol{E}_{\mathrm{rot}}=\dfrac{1}{2}\boldsymbol{\Omega}_B^{\mathrm{T}}(\boldsymbol{I}\boldsymbol{\Omega}_B)$ the rotational kinetic energy and $\boldsymbol{E}_{\mathrm{pot}}=mgz$ the potential energy. So Eq. (18) can be written as

$$\boldsymbol{L}(\varepsilon,\dot{\varepsilon})=\frac{m}{2}\dot{\boldsymbol{\xi}}_I^{\mathrm{T}}\dot{\boldsymbol{\xi}}_I+\frac{1}{2}\boldsymbol{\Omega}_B^{\mathrm{T}}(\boldsymbol{I}\boldsymbol{\Omega}_B)mgz \tag{19}$$

The Euler-Lagrange equations with external forces and torques given as[13]

$$\begin{bmatrix}f_{\xi_I}\\ \tau_B\end{bmatrix}=\frac{\mathrm{d}}{\mathrm{d}t}\left(\frac{\mathrm{d}\boldsymbol{L}}{\mathrm{d}\dot{\varepsilon}}\right)-\frac{\mathrm{d}\boldsymbol{L}}{\mathrm{d}\varepsilon} \tag{20}$$

where $f_{\xi_I}=\boldsymbol{R}\boldsymbol{T}_{B\varepsilon}\ \boldsymbol{R}^3$ is the translational force applied to the quadcopter due to the main thrust and $\tau_B\ \varepsilon\ \boldsymbol{R}^3$ represents the yaw, pitch and roll moments.

Since the Lagrangian does not contain cross terms in the kinetic energies, therefore the Euler-Lagrange equation can be separated into dynamics of $\boldsymbol{\xi}_I$ coordinates and $\boldsymbol{\eta}_I$ coordinates. The Euler-Lagrange equation for the translational motion is written as[1]

$$\frac{\mathrm{d}}{\mathrm{d}t}\left(\frac{\mathrm{d}\boldsymbol{L}_{\mathrm{trans}}}{\mathrm{d}\dot{\boldsymbol{\xi}}_I}\right)-\frac{\mathrm{d}\boldsymbol{L}_{\mathrm{trans}}}{\mathrm{d}\boldsymbol{\xi}_I}=f_{\xi_I} \tag{21}$$

$$f_{\xi_I}=\boldsymbol{R}\boldsymbol{T}_B=m\ddot{\boldsymbol{\xi}}_I+mg\begin{bmatrix}0\\ 0\\ 1\end{bmatrix} \tag{22}$$

which is similar to Eq. (11).

Considering Jacobian matrix $\boldsymbol{J}(\eta)$ from $\boldsymbol{\Omega}_B$ to $\dot{\boldsymbol{\eta}}_I$

$$\boldsymbol{J}(\boldsymbol{\eta}_I)=\boldsymbol{J}=\boldsymbol{W}_{\eta}^{\mathrm{T}}\boldsymbol{I}\boldsymbol{W}_{\eta}=\begin{bmatrix}I_{xx} & 0 & -I_{xx}S_{\theta}\\ 0 & I_{yy}C_{\varphi}^2+I_{zz}S_{\varphi}^2 & (I_{yy}-I_{zz})\,C_{\varphi}S_{\varphi}C_{\theta}\\ -I_{xx}S_{\theta} & (I_{yy}-I_{zz}) & I_{xx}S_{\theta}^2+I_{yy}S_{\varphi}^2C_{\theta}^2+\\ & C_{\varphi}S_{\varphi}C_{\theta} & I_{zz}C_{\varphi}^2C_{\theta}^2\end{bmatrix} \tag{23}$$

The Euler-Lagrange equation for the rotational motion is[1]

$$\frac{\mathrm{d}}{\mathrm{d}t}\left(\frac{\mathrm{d}\boldsymbol{L}_{\mathrm{rot}}}{\mathrm{d}\dot{\boldsymbol{\eta}}_I}\right)-\frac{\mathrm{d}\boldsymbol{L}_{\mathrm{rot}}}{\mathrm{d}\boldsymbol{\eta}_I}=\tau_B \tag{24}$$

$$\boldsymbol{E}_{\mathrm{rot}}=\frac{1}{2}\boldsymbol{\Omega}_B^{\mathrm{T}}(\boldsymbol{I}\boldsymbol{\Omega}_B)=\frac{1}{2}\ddot{\boldsymbol{\eta}}_I^{\mathrm{T}}\boldsymbol{J}\ddot{\boldsymbol{\eta}}_I \tag{25}$$

$$\boldsymbol{J}\ddot{\boldsymbol{\eta}}_I+(\dot{\boldsymbol{J}})\dot{\boldsymbol{\eta}}_I-\frac{1}{2}\frac{\partial}{\partial\boldsymbol{\eta}_I}(\dot{\boldsymbol{\eta}}_I^{\mathrm{T}}\boldsymbol{J}\dot{\boldsymbol{\eta}}_I)=\tau_B \tag{26}$$

Defining $C(\boldsymbol{\eta}_I,\dot{\boldsymbol{\eta}}_I)$, the Coriolis-centripetal term that containing the gyroscopic terms[1].

$$C(\boldsymbol{\eta}_I,\dot{\boldsymbol{\eta}}_I)=(\dot{\boldsymbol{J}})\dot{\boldsymbol{\eta}}_I-\frac{1}{2}\frac{\partial}{\partial\boldsymbol{\eta}_I}(\dot{\boldsymbol{\eta}}_I^{\mathrm{T}}\boldsymbol{J}\dot{\boldsymbol{\eta}}_I) \tag{27}$$

$$\tau_B=\boldsymbol{J}\ddot{\boldsymbol{\eta}}_I+C(\boldsymbol{\eta}_I,\dot{\boldsymbol{\eta}}_I) \tag{28}$$

$$\ddot{\boldsymbol{\eta}}_I=\boldsymbol{J}^{-1}(\tau_B-C(\boldsymbol{\eta}_I,\dot{\boldsymbol{\eta}}_I)) \tag{29}$$

Finally, we get from Eqs. (22), (29)

$$\boldsymbol{\varepsilon}=\begin{bmatrix}m\ddot{x}\\ m\ddot{y}\\ m\ddot{z}\\ \ddot{\varphi}\\ \ddot{\theta}\\ \ddot{\psi}\end{bmatrix}=\begin{bmatrix}T(\sin\varphi\sin\psi+\cos\varphi\cos\psi\sin\theta)\\ T(\cos\varphi\sin\theta\sin\psi+\cos\psi\sin\varphi)\\ T(\cos\theta\cos\varphi)-mg\\ \tilde{\tau}_{\varphi}\\ \tilde{\tau}_{\theta}\\ \tilde{\tau}_{\psi}\end{bmatrix} \tag{30}$$

Eq. (30) is the set of differential equations representing the linear and the angular accelerations of the quadcopter which is analogous to Eq. (17) where $\tilde{\tau}_{\varphi}$, $\tilde{\tau}_{\theta}$ and $\tilde{\tau}_{\psi}$ are the roll moment, the pitch moment and the yaw moment that are associated to the generalized torques τ_{φ}, τ_{θ}, τ_{ψ}, respectively.

1.5 Aerodynamics

To design a quadcopter model with more realistic behavior, the drag forces produced by the air confrontation are merged into the model. The aero-dynamical drag forces can be implemented in quadcopter model by introducing the diagonal drag force coefficients matrix which depends on linear velocities

$$\begin{bmatrix}\ddot{x}\\ \ddot{y}\\ \ddot{z}\end{bmatrix}=-g\begin{bmatrix}0\\ 0\\ 1\end{bmatrix}+\frac{T}{m}\begin{bmatrix}S_{\theta}C_{\varphi}C_{\psi}+S_{\varphi}S_{\psi}\\ S_{\theta}C_{\varphi}S_{\psi}-S_{\varphi}C_{\psi}\\ C_{\theta}C_{\varphi}\end{bmatrix}+\frac{1}{m}\begin{bmatrix}D_x & 0 & 0\\ 0 & D_y & 0\\ 0 & 0 & D_z\end{bmatrix}\begin{bmatrix}\dot{x}\\ \dot{y}\\ \dot{z}\end{bmatrix} \tag{31}$$

where D_x, D_y and D_z are the drag force coefficients of the translational velocities in the x, y and z-directions, respectively, in the inertial frame of reference.

1.6 State space model

The quadcopter model presented by Eqs. (16), (31) can be derived in state space form as

$$\begin{aligned}\dot{\boldsymbol{X}}&=\boldsymbol{A}\boldsymbol{X}+\boldsymbol{B}\boldsymbol{U}\\ \boldsymbol{Y}&=\boldsymbol{C}\boldsymbol{X}+\boldsymbol{D}\boldsymbol{U}\end{aligned} \tag{32}$$

where $\boldsymbol{U}$ is the control input or input vector, and $\boldsymbol{X}$ the state vector is mapped as

$$\boldsymbol{X}=[\varphi\ \dot{\varphi}\ \theta\ \dot{\theta}\ \psi\ \dot{\psi}\ x\ \dot{x}\ y\ \dot{y}\ z\ \dot{z}]^{\mathrm{T}} \tag{33}$$

It can be observed in Eqs. (8), (9) that the total thrust and body torque are main parameters that control quadcopter′s altitude z and attitude $\boldsymbol{\eta}_I$. The x and y positions mostly depend on the pitchangle θ and the rollangle φ. So the controlling variables can be written together as

$$\boldsymbol{U}=\begin{bmatrix}U_1\\ U_2\\ U_3\\ U_4\end{bmatrix}=\begin{bmatrix}T\\ \tau_{\varphi}\\ \tau_{\theta}\\ \tau_{\psi}\end{bmatrix}=\begin{bmatrix}k & k & k & k\\ 0 & -lk & 0 & lk\\ lk & 0 & lk & 0\\ -b & b & -b & b\end{bmatrix}\begin{bmatrix}\omega_1^2\\ \omega_2^2\\ \omega_3^2\\ \omega_4^2\end{bmatrix} \tag{34}$$

The transformation matrix $\boldsymbol{W}_{\eta}$ between the derivative of angular position in the inertial frame $\dot{\varphi},\dot{\theta},\dot{\psi}$ and the angular velocities in body frame p, q, r can be considered as unity matrix, if the perturbations during the flight are small. Then, $\dot{\varphi}\approx p,\dot{\theta}\approx q,\dot{\psi}\approx r$. This assumption is already been verified by simulation tests[10].

The $\boldsymbol{A}$, $\boldsymbol{B}$, $\boldsymbol{C}$ and $\boldsymbol{D}$ matrices in the state space model of the quadcopter can be given as

$$\boldsymbol{A}=\begin{bmatrix}0&1&0&0&0&0&0&0&0&0&0&0\\ 0&0&0&a_1&0&0&0&0&0&0&0&0\\ 0&0&0&1&0&0&0&0&0&0&0&0\\ 0&a_2&0&0&0&0&0&0&0&0&0&0\\ 0&0&0&0&0&1&0&0&0&0&0&0\\ 0&a_3&0&0&0&0&0&0&0&0&0&0\\ 0&0&0&0&0&0&0&0&0&0&0&0\\ 0&0&0&0&0&0&0&a_4&0&0&0&0\\ 0&0&0&0&0&0&0&0&0&0&0&0\\ 0&0&0&0&0&0&0&0&0&a_5&0&0\\ 0&0&0&0&0&0&0&0&0&0&0&0\\ 0&0&0&0&0&0&0&0&0&0&a_6&a_7\end{bmatrix} \tag{35}$$

$$\boldsymbol{B}=\begin{bmatrix}0&0&0&0\\ 0&b_1&0&0\\ 0&0&0&0\\ 0&0&b_2&0\\ 0&0&0&0\\ 0&0&0&b_3\\ 0&0&0&0\\ b_4&0&0&0\\ 0&0&0&0\\ b_5&0&0&0\\ 0&0&0&0\\ b_6&0&0&0\end{bmatrix} \tag{36}$$

$$\boldsymbol{C}=[1\ \ 1\ \ 1\ \ 1\ \ 1\ \ 1\ \ 1\ \ 1\ \ 1\ \ 1\ \ 1\ \ 1] \tag{37}$$

$$\boldsymbol{D}=0 \tag{38}$$

where

$$a_1=\frac{(I_{yy}-I_{zz})}{I_{xx}}\dot{\psi}+\frac{I_m}{I_{xx}}\omega_{\Pi}$$

$$a_2=\frac{(I_{zz}-I_{xx})}{I_{yy}}\dot{\psi}-\frac{I_m}{I_{yy}}\omega_{\Pi}$$

$$a_3=\frac{(I_{xx}-I_{yy})}{I_{zz}}\dot{\theta},a_4=\frac{D_x}{m}$$

$$a_5=\frac{D_y}{m},a_6=\frac{-g}{z},a_7=\frac{D_z}{m}$$

$$b_1=\frac{l}{I_{xx}},b_2=\frac{l}{I_{yy}},b_3=\frac{l}{I_{zz}}$$

$$b_4=\frac{\cos\varphi\sin\theta\cos\psi+\sin\varphi\sin\psi}{m}$$

$$b_5=\frac{\cos\varphi\sin\theta\sin\psi-\sin\varphi\cos\psi}{m}$$

$$b_6=\frac{\cos\varphi\cos\theta}{m},z>0$$

2 Flight Control Design

2.1 Control strategy

Designing the control for a nonlinear underactuated system is not an easy task. The velocities of all four rotors must be regulated in such a manner, that the quadcopter steadily follows the prescribed trajectory. So the effective control strategy must be developed and implemented, which ensures the better tracking and stability performance of the quadcopter. The control strategy which is developed in this paper is presented in Fig. 3, in which six feedback signals x,y,z,θ,φ and ψ are being used for better controlling ability.

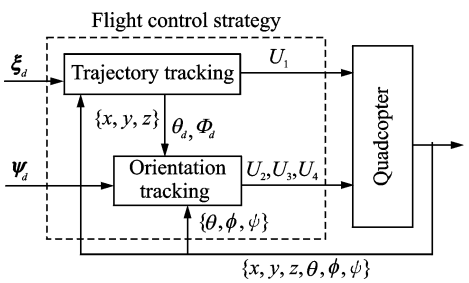

Fig. 3 Flight control design

In this paper, the PD controllers based on the proposed control strategy uses six feedback signals as mentioned above. Whereas the control strategy based on T-S fuzzy controllers is equipped with twelve feedback signals that are x, y,z,θ,φ,ψ and their derivatives.

It can be observed that the four-dimensional control input $\boldsymbol{U}=[U_1\ U_2\ U_3\ U_4]^{\mathrm{T}}$ is projected to follow a three-dimensional translational command $\xi_d=[x_d\quad y_d\quad z_d]^{\mathrm{T}}$.

2.2 PD controller design

The mathematical model of quadcopter presented by Eq. (17) or Eq. (30) is non-linear. In order to design the controller, the model can be linearized around at certain operating point. However, same controller design can be used for a nonlinear model with variations in gains. Using small angle approximations and ignoring the x and y movements terms ($\ddot{x}$ and $\ddot{y}$ becomes around 0 at small angle), the following linearized model is obtained[14]

$$\ddot{z}=-g+\frac{T}{m},\ \ddot{\varphi}=\frac{\tau_\varphi}{m},\ \ddot{\theta}=\frac{\tau_\theta}{m},\ \ddot{\psi}=\frac{\tau_\psi}{m}\quad(39)$$

The original model Eq. (17) or Eq. (30) and linear model Eq. (39) have similar behavior at small variations in θ,φ and ψ[14].

If we take Laplace transform of roll acceleration $\ddot{\varphi}$ in Eq. (39), we get

$$\varphi(s)=\frac{1}{s^2}\ \frac{\tau_\varphi}{m}\quad(40)$$

We can say that the system obtained in Eq. (40) is a double integrator (type-2 system) and ideally, the steady-state error for the type-2 system is null, and this is the reason why the only PD controllers are used.

The PD controllers for altitude and attitude control are as follows

$$\begin{aligned}
u_x&=k_{px}(e_x)+k_{dx}(\dot{e}_x)\\
u_y&=k_{py}(e_y)+k_{dy}(\dot{e}_y)\\
u_z&=k_{pz}(e_z)+k_{dz}(\dot{e}_z)\\
u_\varphi&=k_{p\varphi}(e_\varphi)+k_{d\varphi}(\dot{e}_\varphi)\\
u_\theta&=k_{p\theta}(e_\theta)+k_{d\theta}(\dot{e}_\theta)\\
u_\psi&=k_{p\psi}(e_\psi)+k_{d\psi}(\dot{e}_\psi)
\end{aligned}\quad(41)$$

where $\theta_d=u_x$, $\varphi_d=u_y$ and $\psi_d=0$.

The control laws for the regulation of angular velocities of quadcopter can be given as

$$\begin{cases}
U_1=k_{pz}[e_z(t)]+k_{dz}[\dot{e}_z(t)]\\
U_2=k_{dy}k_{d\varphi}[\ddot{e}_y(t)]+\{k_{dy}k_{p\varphi}+k_{py}k_{d\varphi}\}[\dot{e}_y(t)]+\\
\qquad k_{py}k_{p\varphi}[e_y(t)]-\{k_{d\varphi}[\dot{\varphi}(t)]+k_{p\varphi}[\varphi(t)]\}\\
U_3=k_{dx}k_{d\theta}[\ddot{e}_x(t)]+\{k_{dx}k_{p\theta}+k_{px}k_{d\theta}\}[\dot{e}_x(t)]+\\
\qquad k_{px}k_{p\theta}[e_x(t)]-\{k_{d\theta}[\dot{\theta}(t)]+k_{p\theta}[\theta(t)]\}\\
U_4=k_{p\psi}[e_\psi(t)]+k_{d\psi}[\dot{e}_\psi(t)]
\end{cases}\quad(42)$$

The angular velocity of each rotor can be given in terms of control signals U_1, U_2, U_3, U_4 as follow

$$\omega_1 = \frac{\sqrt{\frac{(-2bU_3 + blU_1 - klU_4}{blk}}}{2}$$

$$\omega_2 = \frac{\sqrt{\frac{(blU_1 - 2bU_2 + klU_4}{blk}}}{2}$$

$$\omega_3 = \frac{\sqrt{\frac{(2bU_3 + blU_1 - klU_4}{blk}}}{2}$$

$$\omega_4 = \frac{\sqrt{\frac{(2bU_2 + blU_1 - klU_4}{blk}}}{2} \tag{43}$$

The gains of all PD controllers are tuned automatically, but after analyzing performance, the gains are slightly modified. These modified gains later are used in simulation to analyze the performance of the controller at different reference inputs and trajectories.

2.3 T-S fuzzy logic controller design

Each fuzzy controller generates one output and takes two inputs. The first input is error input and the other is the rate of change of respective feedback signal, which defines the direction and rate of the parameter to be controlled. For example, the fuzzy controller for altitude controlling will have $e_z = z_d - z$ and $\dot{z}$ as inputs and it generates a controlled output signal U_1 that lifts quadcopter at desired z. Figs. 4, 5 show the membership functions of the fuzzy controller for altitude control, where NB means negative big, NM negative medium, NS negative small, Z zero, PS positive small, PM positive medium, and PB positive big. The 3-dimensional surface plot of the altitude controller that describes the relationship between inputs and output membership functions of the fuzzy logic controller, shown in Fig. 6.

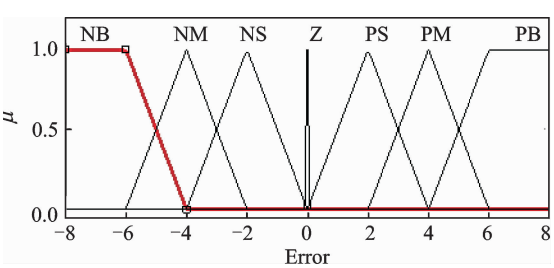

Fig. 4 Membership function plot of error for altitude controller

The Table 1 shows the set of rules for T-S fuzzy controller for altitude tracking. There are 49 rules, by which the controlled output is computed against the given inputs to the fuzzy controller.

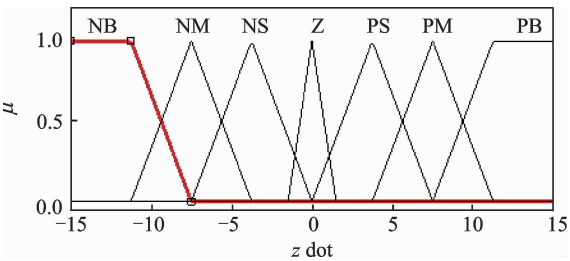

Fig. 5 Membership function plot of $\dot{z}$ for altitude controller

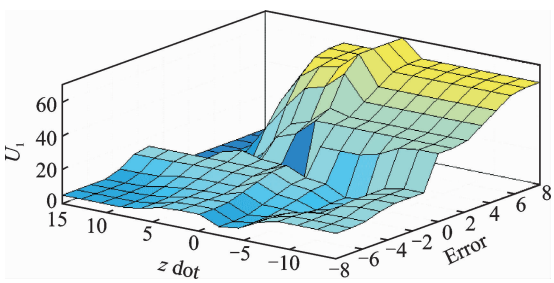

Fig. 6 Surface plot of T-S fuzzy controller for altitude

Table 1 T-S fuzzy rules for altitude controller

e_z	$\dot{z}$						
	PB	PM	PS	Z	NS	NM	NB
PB	80	80	80	80	80	80	80
PM	80	80	80	80	80	80	80
PS	80	40	15	80	80	70	80
Z	47	20	10	60	80	70	80
NS	10	10	10	10	10	42	60
NM	10	10	10	10	10	20	45
NB	10	10	10	10	10	10	10

3 Simulation

The preeminent way to analyze the dynamic behavior of quadcopter under designed control system is to perform its computer-based simulation. The state space model of the quadcopter is not a linear time-invariant (LTI) system, so we cannot use the LTI state space block. Certainly, we need to update the variables in matrices $\boldsymbol{A}$ and $\boldsymbol{B}$ at each instance of time. Therefore, the only way to create the state space model of the quadcopter is by own. So the "matlab function block" is used to generate updated matrices. The quad-

copter model is also configured to simulate the motor cutoff behavior at very low throttle, and most importantly applies the linear relation to control signals and simulates the first order delay for presenting more realistic simulation environment.

The nonlinear model of the quadcopter is simulated under both logic control systems separately at various reference inputs and trajectories to observe the dynamic behavior. The obtained results are discussed below.

3.1 Altitude tracking

The step input $z=5$ m at $t=1$ s is given to flight controller and the following is obtained performance of quadcopter(Fig. 7).

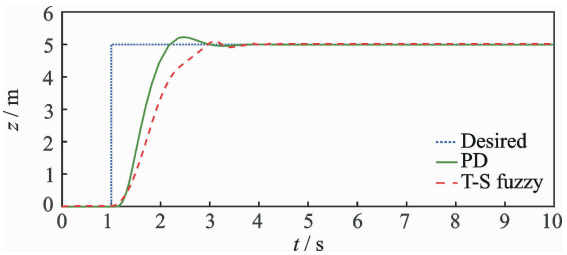

Fig. 7 Altitude tracking performance

As it observable that altitude controller of both control systems lifts the quadcopter smoothly to track the given step input. The PD controller expresses better rise time and settling time, whereas the fuzzy logic controller has better peak overshoot and steady state error performance. Generally, both controllers performed effectively to stabilize the quadcopter at desired height and has given acceptable results.

3.2 *x*-position tracking

Initially, height of 5 m is achieved then the step input is given, to only observe the x-axis tracking performance of the controllers. The step input $x_d=5$ m at $t=3$ s is given control system (Fig. 8).

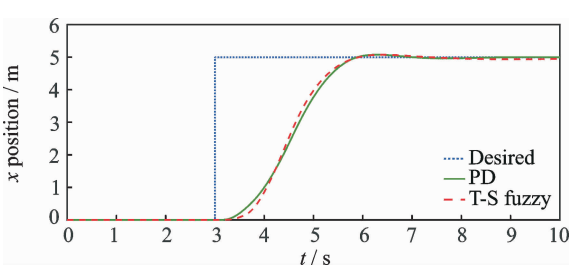

Fig. 8 *x*-position tracking performance

Both the controllers performed effectively to move and stabilize quadcopter at $x_d=5$ m, although rise time and settling time should be improved for some applications. Overall both controllers gave satisfactory results.

3.3 *y*-position tracking

For y-position tracking, the PD controller's performance is observed superior to the T-S fuzzy while tracking, as shown in Fig. 9, though the rising time and settling time of the both controllers should be enhanced to get better results.

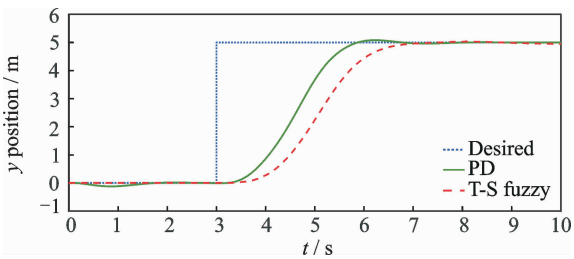

Fig. 9 *y*-position tracking performance

3.4 Attitude tracking

The sine wave of amplitude 1 rad and frequency of 1 rad/s has given as reference input to attitude controllers of both control systems and the results obtained during simulations are presented and discussed below.

Figs. 10—12 show attitude tracking performances of quadcopter under both control systems. It can be observed that there are minor oscillations occurr when quadcopter with T-S fuzzy controller is descending to track sine wave input, but it has almost zero steady state error. On the other hand, PD controller has some initial oscillations, but after some time it gets stable. It has a negligible tracking error of around 0.015 m, when reference input is shifting its phase. Overall attitude controller's performance is considered to be stable

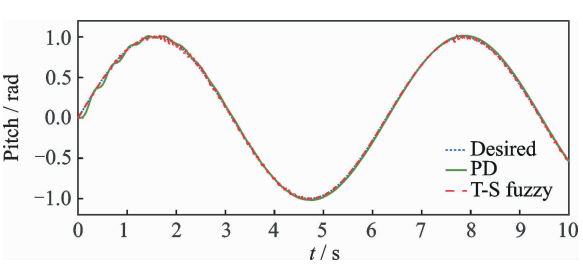

Fig. 10 Pitch angle tracking performance

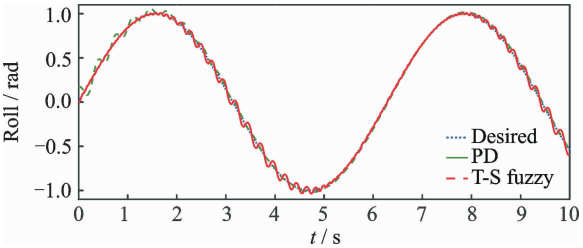

Fig. 11 Roll angle tracking performance

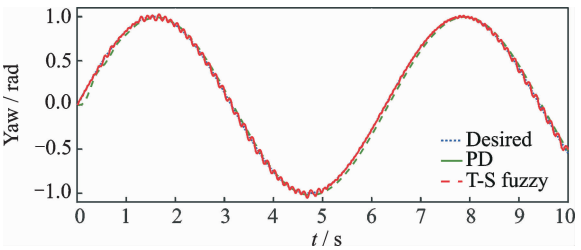

Fig. 12 Yaw angle tracking performance

and acceptable.

4 Conclusions

In this paper, the dynamics of a quadcopter was discussed in details. The full nonlinear model of quadcopter incorporated with aero-dynamical forces was used for the simulation study. The main task of this paper was to design and propose the effective flight control strategy that can deliver the stable tracking performance of the quadcopter UAV. The numerous simulations were conducted in order to analyze and compare the response of quadcopter system under both designed control systems.

Both control systems showed almost similar performance for altitude tracking and x-position tracking. But for y-tracking, the PD based controller performed better than the T-S fuzzy logic controller.

The T-S fuzzy based attitude controller produced minor oscillations while tracking roll-angle, for the period when reference input descending that was due to controller trying to shift velocity from positive to negative while keeping the steady state error at zero. Whereas PD attitude controller′s response was smooth, steady and had a very low steady-state error for all angles. The simulation results depicted a smooth and stable flight response was achieved for both control systems under the proposed control strategy. The presented model and control method was tested and studied only with simulations. A real experimental prototype of a quadcopter should be constructed to achieve more realistic results.

Acknowledgments

This work was supported by the National Natural Science Foundation of China (Nos. 61673209, 61741313, 61304223), the Aeronautical Science Foundation (Nos. 2016ZA52009), the Jiangsu Six Peak of Talents Program (No. KTHY-027); and the Fundamental Research Funds for the Central Universities (Nos. NJ20160026, NS2017015).

References:

[1] LUIS R G C, ALEJANDRO E D L, ROGELIO L, et al. Quad rotorcraft control [M]. London: Springer-Verlag, 2013:23-34.

[2] TEPPO L. Modelling and control of quadcopter: Independent research project in applied mathematics [EB/OL]. 2011-7-1/2015-11-1, http://www.academia.edu/download/46639432/eluu11-public.pdf.

[3] ELRUBY A Y, EL-KHATIB M M, EL-AMARY N H, et al. Dynamic modeling and control of quadrotor vehicle [C]// The 15th International Conference on Applied Mechanics and Mechanical Engineering (AMME). Cairo: AMME, 2012: 280-286.

[4] TAEYOUNG L, MELVIN L N, HARRIS M. Geometric tracking control of a quadcopter UAV on SE (3) [C]// The 49th IEEE Conference on Decision and Control. Atlanta: IEEE, 2010: 5420-5425.

[5] DANIEL G, IONUŢ V, LETIŢIA M, CĂTĂLIN B. Quadcopter control system—modelling and implementation [C]// The 19th International Conference on System Theory, Control and Computing (ICSTCC). Cheile Gradistei: IEEE, 2015: 421-426.

[6] HUNG T N, NADIPURAM R P, CAROL L W, et al. A first course in fuzzy and neural control [M]. [S. l.]:Chapman & Hall/CRC Press, 2003.

[7] OMER C, SEFER K, OKYAY K. Fuzzy logic based approach to design of autonomous landing system for unmanned aerial vehicles [J]. Journal of Intelligent and Robotic Systems, 2011, 64: 1-4.

[8] SIVANANDAM S, SUMATHI S, DEEPA S N. Introduction to fuzzy logic [M]. Britain: Springer, 2007.

[9] YOGIANANDH N, RIAAN S, GLEN B. Quad-rotor unmanned aerial vehicle helicopter modelling &

control [J]. International Journal of Advanced Robotic Systems, 2011, 8(4): 139-149.

[10] SAMIR B, ROLAND S. Full control of a quadcopter [C]// International Conference on Intelligent Robots and Systems. San Diego: IEEE, 2007: 153-158.

[11] CAN D, AYDEMIR A, HAKAN T. Attitude control of a quadcopter [C]// the 4th International Conference on Recent Advances in Space Technologies (RAST). Istanbul: IEEE, 2009: 722-727.

[12] ZHEN Z Y, PU H Z, CHEN Q, et al. Nonlinear intelligent flight control for a quadrotor unmanned helicopter [J]. Transactions of Nanjing University of Aeronautics and Astronautics, 2015, 32(1): 29-34.

[13] PEDRO C, ROGELIO L, ALEJANDRO D. Stabilization of a mini-rotorcraft with four rotors [J]. IEEE Control Systems Magazine, 2005, 25(6): 45-55.

[14] LUIS E R, DAVID F P, JORGE A R. Quadcopter stabilization by using PID controllers [J]. ACTAS: Congreso IEE, 2014, 5: 175-186.

[15] BRESCIANI T. Modeling, identification and control of a quadrotor helicopter [D]. Lund: Lund University, 2008.

[16] SAMIR B, ANDRE N, ROLAND S. PID vs LQ control techniques applied to an indoor micro quadrotor [C]// IEEE/RSJ International Conference on Intelligent Robots and Systems. Sendai: IEEE, 2004: 2451-2456.

[17] ANASTASIA R, IGOR G, HYUN-CHAN C. Adaptive control over quadcopter uav under disturbances [C]// The 14th International Conference on Control, Automation andSystems (ICCAS). Seoul: IEEE, 2014: 386-390.

[18] PAUL P, ROBERT M, PETER C. Modelling and control of a large quadrotor robot [J]. Control Engineering Practice, 2010, 18(7): 691-699.

[19] ABDELKADER A, ABDELHAMID T. Global trajectory tracking control of VTOL-UAVs without linear velocity measurements [J]. Automatica, 2010, 46: 1053-1059.

[20] GUERRERO-CASTELLANOS J F, MARCHAND N, HABLY A, et al. Bounded attitude control of rigid bodies: Real-time experimentation to a quadrotor mini-helicopter [J]. Control Engineering Practice, 2011, 19(1): 790-797.

[21] PINES D J, BOHORQUEZ F. Challenges facing future micro air vehicle development [J]. AIAA Journal of Aircraft, 2006, 43(2): 290-305.

[22] JUN L, YUNTANG L. Dynamic Analysis and PID Control for a Quadrotor [C]// IEEE International Conference on Mechatronics & Automation. Beijing: IEEE, 2011: 573-578.

Mr. **Bhatia Ajeet Kumar** received his B. E. degree in Electronic Engineering from QUEST, Nawabshah, Pakistan in 2009 and M. S. degree in Control Theory and Control Engineering from Nanjing University of Aeronautics and Astronautics (NUAA), China, in 2017. His research interest includes flight control and adaptive control methods.

Prof. **Jiang Ju** received his M. S. and Ph. D. degrees in navigation, guidance and control from Beijing University of Aeronautics and Astronautics, Beijing, China, in 1988 and 2007. He is currently a professor at Nanjing University of Aeronautics and Astronautics. His research interests includes advanced flight control of aircraft systems.

Dr. **Zhen Ziyang** received his Ph. D. degree from the Nanjing University of Aeronautics and Astronautics (NUAA) in 2010. He worked at the University of Virginia, U. S. A. as a visiting scholar from February 2015 to February 2016. Currently, he is working at NUAA as an associate professor. His research interests includes advanced flight control of carrier-based aircrafts, hypersonic aircrafts and UAVs formation control, adaptive control and preview control.

(Executive Editor: Zhang Bei)